http://www.applmathmech.cn

含椭圆孔有限大二十面体准晶板平面弹性问题的边界元分析*

王会苹[1]，　王桂霞[1,2]，　陈德财[1]

（1. 内蒙古师范大学 数学科学学院，呼和浩特 010022；
2. 内蒙古自治区应用数学中心，呼和浩特 010022）

摘要： 基于扩展的 Stroh 方法，对含椭圆孔有限大二十面体准晶板平面弹性问题进行边界元分析.首先利用扩展的 Stroh 方法，研究了二十面体准晶的 Green 函数，得到了含椭圆孔无限大二十面体准晶平面弹性问题位移和应力的基本解.利用该基本解，通过加权余量法建立了区域内积分方程和边界积分方程，并采用线性插值函数及 Gauss 积分对含未知量的边界积分方程和区域内积分方程分别进行离散,得到了离散格式.进一步，对椭圆孔的孔边应力进行了数值求解，并将有限大板的数值结果与无限大板的解析解进行了对比验证，说明当板与椭圆孔尺寸之比小于某下限值时，不能用无限大板的解析解对有限大板进行分析.最后，分析了在垂向拉伸作用下，板的大小、孔口尺寸及倾斜角度对孔边应力的影响.结果表明：板的尺寸沿垂直拉伸方向变化对孔边应力的影响更明显；随着椭圆孔尺寸的增加，孔边应力集中现象越明显；若长轴垂直拉伸方向，椭圆孔倾斜会减缓孔边应力集中程度.

关　键　词： 二十面体准晶；　Stroh 方法；　椭圆孔；　有限尺寸；　应力集中系数
中图分类号： O343.1；O343.4；O241.82　　**文献标志码：** A　　DOI：10.21656/1000-0887.440241

Boundary Element Analysis for the Plane Elasticity Problems of Finite Icosahedral Quasicrystal Plates Containing Elliptical Holes

WANG Huiping[1]，　WANG Guixia[1,2]，　CHEN Decai[1]

（1. *College of Mathematics Science*, *Inner Mongolia Normal University*, *Hohhot* 010022, *P.R.China*;
2. *Inner Mongolia Center of Applied Mathematics*, *Hohhot* 010022, *P.R.China*）

Abstract: Based on the extended Stroh method, a boundary element analysis was conducted for the plane elasticity problem of finite-sized icosahedral quasicrystal plates with elliptical holes. Firstly, the extended Stroh method was used to study Green's function for the icosahedral quasicrystal, to obtain the fundamental solutions of displacements and stresses of the plane elasticity problem about infinite-sized icosahedral quasicrystal plates with elliptical holes. With these fundamental solutions, the weighted residual method was employed to

* **收稿日期：** 2023-08-14；**修订日期：** 2023-12-12
基金项目： 国家自然科学基金(11962026)；内蒙古自治区自然科学基金重点项目(2022ZD05)；内蒙古自治区高校科研项目(NJZZ21003)
作者简介： 王会苹(1999—)，女，硕士生(E-mail：whp7464@163.com)；
王桂霞(1968—)，女，教授，博士(通讯作者. E-mail：nsdwgx@126.com).
引用格式： 王会苹，王桂霞，陈德财. 含椭圆孔有限大二十面体准晶板平面弹性问题的边界元分析[J]. 应用数学和力学，2024，**45**(4)：400-415.

establish the integral equations within the domain and on the boundary, and the linear interpolation functions and the Gaussian integration were used to discretize the boundary integral equations and the domain integral equations with unknown variables, respectively. Furthermore, the stress at the hole boundary was numerically solved, and the numerical results of the finite-sized plate were compared with the analytical solution of the infinite-sized plate to demonstrate that, the analytical solution of the infinite-sized plate cannot be used for the analysis of the finite-sized plate with the ratio of the plate size to the hole size below a certain threshold. Finally, the effects of the plate size, the hole size, and the inclination angle on the stress at the hole boundary were analyzed under tensile loading in the vertical direction. The results show that, the variation of the plate size along the vertical tensile direction has a more significant effect on the stress at the hole boundary. As the elliptical hole size increases, the stress concentration phenomenon becomes more pronounced. If the major axis is perpendicular to the vertical tensile direction, the inclination of the elliptical hole will mitigate the degree of stress concentration at the hole boundary.

Key words: icosahedral quasicrystal; Stroh method; elliptical hole; finite size; stress concentration factor

0 引　　言

在传统的凝聚态物理学中,固体一般被分为晶体和非晶体两大类,1984 年 Shechtman 等发现了一种不同于传统晶体和非晶体的新固体——准晶[1-2].至今已发现的 200 多种准晶中,二十面体准晶几乎占一半[3].目前,准晶热障涂层已经应用到飞机和汽车的发动机等部件中,发动机热障涂层技术是解决燃油汽车节能减排问题的有效手段之一.此外,材料开孔现象很常见,如机械结构中的螺栓孔及铆钉孔等.准晶构件对孔洞等缺陷非常敏感,在外载荷作用下,含孔洞的准晶构件会出现应力集中,应力集中在孔边诱发裂纹导致材料断裂破坏.研究准晶缺陷力学行为,提高结构的可靠性,对准晶器件的开发具有重要的指导意义.

在实际工程应用中,构件的尺寸是有限的.对于有限大板的缺陷问题,目前多使用数值方法进行近似求解,常用的数值方法包括有限差分法、有限元法及边界元法.有限差分法只适用于解决规则区域的问题,对于孔洞等缺陷无法进行均匀的网格划分.有限元方法的计算量大,对于应力变化剧烈的含孔板计算精度低.边界元方法作为一种半解析半数值方法,只需对边界离散,区域内的有关物理量可由解析式的离散形式直接求得,离散化误差仅来源于边界,因此提高了计算精度.将区域的边界分割成边界单元,与对整个区域进行网格剖分的解法相比,具有输入数据少、计算时间短等优点,特别适用于有限大体含孔洞缺陷的问题.如果只侧重考虑孔边的应力或位移,不讨论区域内的物理量,边界元方法可以不必计算区域内相关物理量的值,显然能提高计算效率.边界元法已经被广泛应用于求解结构力学、声学、电磁场等问题.Hwu 等利用边界元法求解了含椭圆孔各向异性弹性板的断裂力学问题,并将椭圆孔退化到裂纹,计算了裂纹尖端处的应力强度因子[4];舒小敏等利用边界元法求解了三维弹性摩擦接触问题[5];Xu 等利用边界元法探讨了含斜椭圆孔以及两个圆孔的压电材料的断裂力学问题[6];Liang 等利用边界元法解决了含中心裂纹压电材料的断裂力学问题[7];袁彦鹏利用边界元法研究了一维六方热准晶复合材料的界面断裂力学问题[8];陈帅利用边界元法研究了一维六方准晶及一维六方压电准晶复合材料的界面断裂力学问题[9];潘先云等利用双互易边界元法求解了非齐次弹性力学问题[10].

二十面体准晶是三维准晶的一种,根据某些具体构型,即使其弹性问题可以化成一个平面弹性问题与一个反平面声子场弹性问题的叠加,平面问题的最终控制方程仍非常复杂,求解难度很大[3].翟婷等研究了在平面集中力和无穷远处均匀拉伸应力作用下,带圆弧形界面刚性线夹杂的三维二十面体准晶的平面弹性问题[11];Wang 等研究了三维二十面体准晶中球形夹杂问题[12];祝爱玉等研究了三维二十面体准晶平面弹性理论[3,13-17];Li 通过引进应力势函数,利用扩展的 Stroh 方法,讨论了含椭圆孔口三维二十面体准晶的广义二维问题[18],为数值计算奠定了基础.对于含孔洞或裂纹无限大板解析解的研究成果比较丰富[19-27],而对于有限大准晶板平面弹性问题,目前尚缺乏解析解.范天佑等用有限元方法求解了平面八次对称准晶受内压圆筒问题以及Ⅰ型 Griffith 裂纹问题[2,28],并利用有限差分法研究了点群 10 mm 的十次对称二维准晶及三维二

十面体准晶中裂纹对冲击载荷的响应和裂纹快速传播问题[3,29-30].杨连枝等建立了二十面体准晶三维边值问题及二十面体准晶弹性变形问题的有限元法,研究了包含裂纹的二十面体准晶板的断裂行为[31-32].本文对含椭圆孔的有限大二十面体准晶板进行边界元分析,讨论了耦合常数、椭圆孔尺寸及椭圆孔倾斜程度对声子场和相位子场孔边应力的影响,并将椭圆孔退化到裂纹,计算裂纹尖端应力强度因子.

1 基本方程及 Stroh 公式

由二十面体准晶的平面弹性理论可知[2], 其声子场与相位子场的应力-应变关系满足广义 Hooke 定律

$$\sigma_{ij} = C_{ijkl}\varepsilon_{ij} + R_{ijkl}\omega_{ij},\ H_{ij} = K_{ijkl}\omega_{kl} + R_{klij}\varepsilon_{kl}, \tag{1}$$

变形几何方程

$$\varepsilon_{ij} = \frac{1}{2}\left(\frac{\partial u_i}{\partial x_j} + \frac{\partial u_j}{\partial x_i}\right),\ \omega_{ij} = \frac{\partial w_i}{\partial x_j},\qquad i,j = 1,2,3, \tag{2}$$

及不计体力的平衡方程

$$\frac{\partial \sigma_{ij}}{\partial x_j} = 0,\ \frac{\partial H_{ij}}{\partial x_j} = 0,\qquad i,j = 1,2,3, \tag{3}$$

其中, $\sigma_{ij},\varepsilon_{ij},C_{ijkl},u_i$ 分别为声子场应力、应变、弹性常数和位移;$H_{ij},\omega_{ij},K_{ijkl},w_i$ 分别为相位子场应力、应变、弹性常数和位移;R 为声子场-相位子场耦合弹性常数.

假设 z 轴为二十面体准晶的五重对称轴,讨论椭圆孔面沿周期方向(z 方向) 穿透整个材料的情况.从几何上看,构形不随 z 变化,在这种情况下,

$$\frac{\partial}{\partial z} = 0. \tag{4}$$

将式(1)和式(2)代入式(3),得到二十面体准晶的平面弹性问题的控制方程:

$$\begin{cases}
\mu\nabla^2 u_x + (\lambda+\mu)\dfrac{\partial}{\partial x}\nabla\cdot\boldsymbol{u} + R\left(\dfrac{\partial^2 w_x}{\partial x^2} + 2\dfrac{\partial^2 w_y}{\partial x\partial y} - \dfrac{\partial^2 w_x}{\partial y^2}\right) = 0,\\
\mu\nabla^2 u_y + (\lambda+\mu)\dfrac{\partial}{\partial y}\nabla\cdot\boldsymbol{u} + R\left(\dfrac{\partial^2 w_y}{\partial x^2} - 2\dfrac{\partial^2 w_x}{\partial x\partial y} - \dfrac{\partial^2 w_y}{\partial y^2}\right) = 0,\\
\mu\nabla^2 u_z + R\left(\dfrac{\partial^2 w_x}{\partial x^2} - 2\dfrac{\partial^2 w_y}{\partial x\partial y} - \dfrac{\partial^2 w_x}{\partial y^2} + \nabla^2 w_z\right) = 0,\\
K_1\nabla^2 w_x + K_2\left(\dfrac{\partial^2 w_z}{\partial x^2} - \dfrac{\partial^2 w_z}{\partial y^2}\right) + R\left(\dfrac{\partial^2 u_x}{\partial x^2} - 2\dfrac{\partial^2 u_y}{\partial x\partial y} - \dfrac{\partial^2 u_x}{\partial y^2} + \dfrac{\partial^2 u_z}{\partial x^2} - \dfrac{\partial^2 u_z}{\partial y^2}\right) = 0,\\
K_1\nabla^2 w_y - 2K_2\dfrac{\partial^2 w_z}{\partial x\partial y} + R\left(\dfrac{\partial^2 u_y}{\partial x^2} + 2\dfrac{\partial^2 u_x}{\partial x\partial y} - \dfrac{\partial^2 u_y}{\partial y^2} - 2\dfrac{\partial^2 u_z}{\partial x\partial y}\right) = 0,\\
(K_1 - K_2)\nabla^2 w_z + K_2\left(\dfrac{\partial^2 w_x}{\partial x^2} - 2\dfrac{\partial^2 w_y}{\partial x\partial y} - \dfrac{\partial^2 w_y}{\partial y^2}\right) + R\nabla^2 u_z = 0,
\end{cases} \tag{5}$$

其中

$$\nabla^2 = \frac{\partial^2}{\partial x^2} + \frac{\partial^2}{\partial y^2},\ \boldsymbol{u} = (u_x,u_y),\ \nabla\cdot\boldsymbol{u} = \frac{\partial u_x}{\partial x} + \frac{\partial u_y}{\partial y}.$$

令 $z = x_1 + px_2$, 引入广义位移分量

$$\boldsymbol{u} = \{u_1,u_2,u_3,w_1,w_2,w_3\}^{\mathrm{T}} = \boldsymbol{a}f(z), \tag{6}$$

其中, $f(z)$ 为任意函数, p 是待求复数, $\boldsymbol{a}$ 为列向量.由式(6)和式(5)得

$$\{\boldsymbol{Q} + p(\boldsymbol{R} + \boldsymbol{R}^{\mathrm{T}}) + p^2\boldsymbol{T}\}\boldsymbol{a} = \boldsymbol{0}, \tag{7}$$

其中

$$\boldsymbol{Q}=\begin{bmatrix}\lambda+2\mu & 0 & 0 & R & 0 & 0\\ 0 & \mu & 0 & 0 & R & 0\\ 0 & 0 & \mu & R & 0 & R\\ R & 0 & R & K_1 & 0 & K_2\\ 0 & R & 0 & 0 & K_1 & 0\\ 0 & 0 & R & K_2 & 0 & K_1-K_2\end{bmatrix},\ \boldsymbol{R}=\begin{bmatrix}0 & \lambda & 0 & 0 & R & 0\\ \mu & 0 & 0 & -R & 0 & 0\\ 0 & 0 & 0 & 0 & -R & 0\\ 0 & -R & 0 & 0 & 0 & 0\\ R & 0 & -R & 0 & 0 & -K_2\\ 0 & 0 & 0 & 0 & -K_2 & 0\end{bmatrix},$$

$$\boldsymbol{T}=\begin{bmatrix}\mu & 0 & 0 & -R & 0 & 0\\ 0 & \lambda+2\mu & 0 & 0 & -R & 0\\ 0 & 0 & \mu & -R & 0 & R\\ -R & 0 & -R & K_1 & 0 & -K_2\\ 0 & -R & 0 & 0 & K_1 & 0\\ 0 & 0 & R & -K_2 & 0 & K_1-K_2\end{bmatrix}. \tag{8}$$

式(7)的特征根记为 $p_\alpha(\alpha=1,2,3,4,5,6)$,$p_\alpha$ 为 6 个不同的复特征根.由应变能的正定性可知 p_α 含有正虚部, $\boldsymbol{a}$ 是对应的特征向量.

引入应力函数 $\boldsymbol{\psi}=\boldsymbol{b}f(z)$,并令 $\boldsymbol{b}=(\boldsymbol{R}^{\mathrm{T}}+p\boldsymbol{T})\boldsymbol{a}$, 则不含缺陷无限大板平面问题位移和应力的通解分别表示为

$$\boldsymbol{u}=2\mathrm{Re}\{\boldsymbol{A}\langle f(z_*)\rangle\ \boldsymbol{q}\},\ \boldsymbol{\psi}=2\mathrm{Re}\{\boldsymbol{B}\langle f(z_*)\rangle\ \boldsymbol{q}\}, \tag{9}$$

其中, $\boldsymbol{A}=[a_1,a_2,a_3,a_4,a_5,a_6]$,$\boldsymbol{B}=[b_1,b_2,b_3,b_4,b_5,b_6]$,$\boldsymbol{q}=\{q_1,q_2,q_3,q_4,q_5,q_6\}^{\mathrm{T}}$.

进一步考虑含椭圆孔无限大板在点 $x^*(x_1^*,x_2^*)$ 受一集中力 $\hat{\boldsymbol{p}}$, 如图 1 所示.

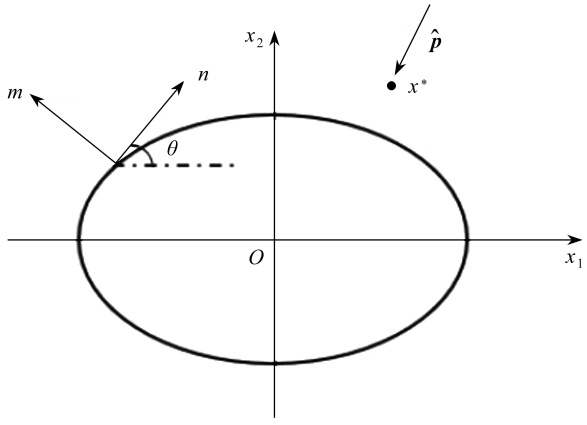

图 1 构型及受力情况

Fig. 1 The configuration and the force

椭圆孔边界用参数方程 $x_1=a\cos\varphi$,$x_2=b\sin\varphi$ 表示,$\varphi\in[0,2\pi]$,a,b 分别为椭圆的长半轴和短半轴.当椭圆孔不受力时,边界条件为

$$\begin{cases}\boldsymbol{t}_m=\boldsymbol{\psi}_{,n}=\boldsymbol{0},\ \oint_C \mathrm{d}\boldsymbol{\psi}=\hat{\boldsymbol{p}},\ \oint_C \mathrm{d}\boldsymbol{u}=\boldsymbol{0},\\ \sigma_{ij}\to 0,\ H_{ij}\to 0,\end{cases} \tag{10}$$

其中, C 表示椭圆边界.

利用保角映射

$$z_\alpha=\frac{1}{2}\left[(a-\mathrm{i}bp_\alpha)\zeta_\alpha+(a+\mathrm{i}bp_\alpha)\frac{1}{\zeta_\alpha}\right], \tag{11}$$

将 z_α 平面内椭圆孔外部的区域映射到 ζ_α 平面内单位圆外部.结合式(9)和式(11),含椭圆孔无限大板平面问题的通解为[4]

$$\begin{cases}\boldsymbol{u}=2\mathrm{Re}\{\boldsymbol{A}\langle f_0(z_*)\rangle\,\boldsymbol{q}_0\}+2\sum\limits_{\beta=1}^{6}\mathrm{Re}\{\boldsymbol{A}\langle f_\beta(z_*)\rangle\,\boldsymbol{q}_\beta\},\\ \boldsymbol{\psi}=2\mathrm{Re}\{\boldsymbol{B}\langle f_0(z_*)\rangle\,\boldsymbol{q}_0\}+2\sum\limits_{\beta=1}^{6}\mathrm{Re}\{\boldsymbol{B}\langle f_\beta(z_*)\rangle\,\boldsymbol{q}_\beta\},\end{cases}\tag{12}$$

其中

$$\begin{cases}\langle f_k(z_*)\rangle=\mathrm{diag}[f_k(z_1),f_k(z_2),f_k(z_3),f_k(z_4),f_k(z_5),f_k(z_6)], & k=1,2,3,4,5,6,\\ f_0(z_\alpha)=\ln(\zeta_\alpha-\zeta_\alpha^*),\ f_\beta(z_\alpha)=\ln(\zeta_\alpha^{-1}-\bar{\zeta}_\beta^*), & \alpha,\beta=1,2,3,4,5,6,\\ \zeta_\alpha=\dfrac{z_\alpha+\sqrt{z_\alpha^2-a^2-p_\alpha^2b^2}}{a-\mathrm{i}p_\alpha b},\ \zeta_\alpha^*=\dfrac{z_\alpha^*+\sqrt{z_\alpha^{*\,2}-a^2-p_\alpha^2b^2}}{a-\mathrm{i}p_\alpha b},\ z_\alpha^*=x_1^*+p_\alpha x_2^*.\end{cases}\tag{13}$$

为进一步确定式(12)中的 $\boldsymbol{q}_0$ 和 $\boldsymbol{q}_\beta$, 对式(13)求导得

$$\begin{cases}\dfrac{\partial}{\partial n}\langle f_0(z_*)\rangle\Big|_\Gamma=\mathrm{diag}[c_1,c_2,c_3,c_4,c_5,c_6]=\sum\limits_{\beta=1}^{6}c_\beta\boldsymbol{I}_\beta,\\ \dfrac{\partial}{\partial n}\langle f_\beta(z_*)\rangle\Big|_\Gamma=\bar{c}_\beta\boldsymbol{I},\end{cases}\tag{14}$$

其中

$$c_\beta=\frac{-\mathrm{i}\mathrm{e}^{\mathrm{i}\varphi}}{\rho(\mathrm{e}^{\mathrm{i}\varphi}-\zeta_\beta^*)}.\tag{15}$$

将式(14)和式(12)代入边界条件得

$$\begin{cases}\sum\limits_{\beta=1}^{6}\mathrm{Re}\{c_\beta\boldsymbol{B}\boldsymbol{I}_\beta\boldsymbol{q}_0+\bar{c}_\beta\boldsymbol{B}\boldsymbol{I}_\beta\boldsymbol{q}_\beta\}=0,\\ \boldsymbol{B}\boldsymbol{q}_0-\overline{\boldsymbol{B}\boldsymbol{q}_0}=\dfrac{1}{2\pi\mathrm{i}}\hat{\boldsymbol{p}},\ \boldsymbol{A}\boldsymbol{q}_0-\overline{\boldsymbol{A}\boldsymbol{q}_0}=\boldsymbol{0}.\end{cases}\tag{16}$$

易知

$$\boldsymbol{q}_0=\frac{1}{2\pi\mathrm{i}}\boldsymbol{A}^{\mathrm{T}}\hat{\boldsymbol{p}},\ \boldsymbol{q}_\beta=-\boldsymbol{B}^{-1}\bar{\boldsymbol{B}}\boldsymbol{I}_\beta\bar{\boldsymbol{q}}_0.\tag{17}$$

将式(17)代入式(12),可得含椭圆孔无限大二十面体准晶的 Green 函数为

$$\begin{cases}\boldsymbol{u}=\dfrac{1}{\pi}\mathrm{Im}\left\{\boldsymbol{A}\left[\langle\ln(\zeta_\alpha-\zeta_\alpha^*)\rangle\boldsymbol{A}^{\mathrm{T}}+\sum\limits_{\beta=1}^{6}\langle\ln(\zeta_\alpha^{-1}-\bar{\zeta}_\beta^*)\rangle\boldsymbol{B}^{-1}\bar{\boldsymbol{B}}\boldsymbol{I}_\beta\bar{\boldsymbol{A}}^{\mathrm{T}}\right]\right\}\hat{\boldsymbol{p}},\\ \boldsymbol{\psi}=\dfrac{1}{\pi}\mathrm{Im}\left\{\boldsymbol{B}\left[\langle\ln(\zeta_\alpha-\zeta_\alpha^*)\rangle\boldsymbol{A}^{\mathrm{T}}+\sum\limits_{\beta=1}^{6}\langle\ln(\zeta_\alpha^{-1}-\bar{\zeta}_\beta^*)\rangle\boldsymbol{B}^{-1}\bar{\boldsymbol{B}}\boldsymbol{I}_\beta\bar{\boldsymbol{A}}^{\mathrm{T}}\right]\right\}\hat{\boldsymbol{p}}.\end{cases}\tag{18}$$

2 边界条件及边界积分方程

含椭圆孔有限尺寸准晶试样如图 2 所示,孔口中心与试样中心重合.板宽为 W,高为 H,椭圆长半轴为 a,短半轴为 b.试样两端施加 $\hat{\sigma}=1$ GPa 的拉伸力,椭圆孔边不受力.

相应的边界条件为

$$\begin{cases}u_i=\bar{u}_i,\ w_i=\bar{w}_i, & x_i\in\Gamma_1,\\ t_i=\sigma_{ij}m_j=\bar{t}_i,\ h_i=H_{ij}m_j=\bar{h}_i, & x_i\in\Gamma_2,\end{cases}\tag{19}$$

其中,$\Gamma_1\cup\Gamma_2=\Gamma$,$\Gamma$ 为该构型的整体边界,Γ_1,Γ_2 为任意边界,$\bar{u}_i$,$\bar{t}_i$,$\bar{w}_i$,$\bar{h}_i$ 为给定的初值.初始条件给定位移的所有离散节点的集合记为 Γ_1,初始条件给定力加载的所有离散节点的集合记为 Γ_2.

引入记号

$$u_{4,j}\doteq\omega_{1j}=2\Xi_{4j},\ u_{5,j}\doteq\omega_{2j}=2\Xi_{5j},\ u_{6,j}\doteq\omega_{3j}=2\Xi_{6j},$$

将式(1)—(3)记为

$$Y_{IJ} = C_{IJKL}\Xi_{KL},\ \Xi_{IJ} = \frac{1}{2}(u_{I,J} + u_{J,I}),\ Y_{IJ,J} = 0; \tag{20}$$

式(19)记为

$$\begin{cases} u_I = \bar{u}_I, & x_I \in \Gamma_1, \\ t_I = Y_{IJ}m_J = \bar{t}_I, & x_I \in \Gamma_2, \end{cases} \tag{21}$$

其中,当 $I \leqslant 3$ 时,$Y_{IJ} = \sigma_{ij}$,$\Xi_{IJ} = \varepsilon_{ij}$;当 $I > 3$ 时,$Y_{IJ} = H_{ij}$,$\Xi_{IJ} = \omega_{ij}$,$I,J,K,L = 1,2,3,4,5,6$;且当 $I > 3$ 时,$u_{J,I} = 0$;当 $J,L > 3$ 时,Y_{IJ},C_{IJKL},Ξ_{KL} 为 0.

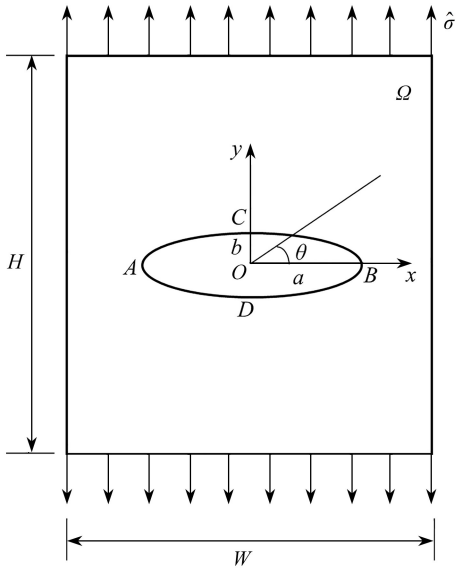

图 2 含椭圆孔的试样

Fig. 2 The specimen containing an elliptical hole

式(20)和式(21)构成微分方程边值问题,其定解问题弱形式相应的加权余量表达式为

$$\iint_{\Omega} Y_{IJ,J}\bar{\omega}_I \mathrm{d}\Omega + \int_{\Gamma_1}(u_I - \bar{u}_I)\bar{\omega}_{\Gamma_{1I}}\mathrm{d}\Gamma + \int_{\Gamma_2}(t_I - \bar{t}_I)\bar{\omega}_{\Gamma_{2I}}\mathrm{d}\Gamma = 0, \tag{22}$$

其中,$\bar{\omega}_I$,$\bar{\omega}_{\Gamma_{1I}}$,$\bar{\omega}_{\Gamma_{2I}}$ 分别为域 Ω 以及边界 Γ_1,Γ_2 的权函数,域 Ω 为椭圆孔至边界之间的区域.现取基本解 u_I^* 为域 Ω 的权函数,即 $\bar{\omega}_I = u_I^*$,边界权函数取

$$\bar{\omega}_{\Gamma_{1I}} = t_I^* = Y_{IJ}^* m_J,\ \bar{\omega}_{\Gamma_{2I}} = -u_I^*. \tag{23}$$

将基本解 u_I^* 及式(23)代入式(22),得

$$\iint_{\Omega} Y_{IJ,J}u_I^* \mathrm{d}\Omega + \int_{\Gamma_1}(u_I - \bar{u}_I)t_I^* \mathrm{d}\Gamma - \int_{\Gamma_2}(t_I - \bar{t}_I)u_I^* \mathrm{d}\Gamma = 0, \tag{24}$$

应用散度定理将上述方程整理为

$$\iint_{\Omega} Y_{IJ,J}^* u_I \mathrm{d}\Omega + \int_{\Gamma_1} t_I u_I^* \mathrm{d}\Gamma_1 + \int_{\Gamma_2} \bar{t}_I u_I^* \mathrm{d}\Gamma_2 - \int_{\Gamma_1} \bar{u}_I t_J^* \mathrm{d}\Gamma_1 - \int_{\Gamma_2} u_I t_J^* \mathrm{d}\Gamma_2 = 0. \tag{25}$$

利用

$$Y_{IJ,J}^* + \Delta(\xi)\delta_{IJ} = 0,$$

并将 Γ_1 上的 $\bar{u}_I$ 记为 u_I,Γ_2 上的 $\bar{t}_I$ 记为 t_I,u_I^* 和 t_I^* 记为 u_{IJ}^* 和 t_{IJ}^*,由式(25)可得区域内的积分方程:

$$u_I(\xi) + \int_{\Gamma} u_I t_{IJ}^* \mathrm{d}\Gamma = \int_{\Gamma} t_I u_{IJ}^* \mathrm{d}\Gamma.$$

将区域内点 ξ 向边界逼近[33],可得边界积分方程:

$$D_{IJ}(\xi)u_I(\xi) + \int_{\Gamma} u_I(x)t_{IJ}^*(\xi,x)\mathrm{d}\Gamma = \int_{\Gamma} t_I(x)u_{IJ}^*(\xi,x)\mathrm{d}\Gamma. \tag{26}$$

若在点 $\xi = (x_1,x_2)$ 施加单位力 $\hat{\boldsymbol{p}} = (1,0,0,0,0,0)$,由式(18)中的 $\boldsymbol{u}$ 直接得到 u_{1J}^*,而 t_{1J}^* 由 $\partial\boldsymbol{\psi}/\partial n$ 得到.类

似地,可以得到 u_{IJ}^{*} 和 t_{IJ}^{*},$I \neq 1$.将 $u_I = 1$ 和 $t_I = 0$ 代入式(26),可得

$$D_{IJ}(\xi) = -\int_{\Gamma} t_{IJ}^{*}(\xi, x)\,\mathrm{d}\Gamma(x)\,. \tag{27}$$

将边界积分方程(26)写成矩阵形式

$$\boldsymbol{D}(\xi)\boldsymbol{u}(\xi) + \int_{\Gamma} \boldsymbol{T}^{*}(\xi, x)\boldsymbol{u}(x)\,\mathrm{d}\Gamma(x) = \int_{\Gamma} \boldsymbol{U}^{*}(\xi, x)\boldsymbol{t}(x)\,\mathrm{d}\Gamma(x)\,, \tag{28}$$

其中,$\boldsymbol{t}$ 和 $\boldsymbol{u}$ 是长度为 6 的列向量,$\boldsymbol{D} = (D_{IJ})$,$\boldsymbol{U}^{*} = (u_{IJ}^{*})$,$\boldsymbol{T}^{*} = (t_{IJ}^{*})$ 为六阶方阵,且

$$\boldsymbol{U}^{*} = \frac{1}{\pi}\,\mathrm{Im}\left\{\boldsymbol{A}\left[\langle \ln(\zeta_\alpha - \zeta_\alpha^{*})\rangle \boldsymbol{A}^{\mathrm{T}} + \sum_{\beta=1}^{6} \langle \ln(\zeta_\alpha^{-1} - \bar{\zeta}_\beta^{*})\rangle \boldsymbol{B}^{-1}\bar{\boldsymbol{B}}\boldsymbol{I}_\beta\bar{\boldsymbol{A}}^{\mathrm{T}}\right]\right\},$$

$$\boldsymbol{T}^{*} = \frac{1}{\pi}\,\mathrm{Im}\left\{\boldsymbol{B}\left\langle \frac{2\zeta_\alpha^{2}(\partial x_1/\partial n + p_\alpha \partial x_2/\partial n)}{(\zeta_\alpha - \zeta_\alpha^{*})[(a - \mathrm{i}p_\alpha b)\zeta_\alpha^{2} - (a + \mathrm{i}p_\alpha b)]}\right\rangle \boldsymbol{A}^{\mathrm{T}}\right\} +$$

$$\frac{1}{\pi}\sum_{\beta=1}^{6}\,\mathrm{Im}\left\{\boldsymbol{B}\left\langle \frac{-2\zeta_\alpha(\partial x_1/\partial n + p_\alpha \partial x_2/\partial n)}{(1 - \zeta_\alpha\bar{\zeta}_\beta^{*})[(a - \mathrm{i}p_\alpha b)\zeta_\alpha^{2} - (a + \mathrm{i}p_\alpha b)]}\right\rangle \boldsymbol{B}^{-1}\bar{\boldsymbol{B}}\boldsymbol{I}_\beta\bar{\boldsymbol{A}}^{\mathrm{T}}\right\}$$

为边界元法所需的位移基本解和应力基本解.

3 离散化与求解过程

采用线性单元对边界积分方程(28)进行离散,离散后的边界积分方程为

$$\boldsymbol{D}(\xi)\boldsymbol{u}(\xi) + \sum_{m=1}^{M}\{\hat{\boldsymbol{Y}}_m^{(1)}(\xi)\boldsymbol{u}_m^{(1)} + \hat{\boldsymbol{Y}}_m^{(2)}(\xi)\boldsymbol{u}_m^{(2)}\} = \sum_{m=1}^{M}\{\boldsymbol{G}_m^{(1)}(\xi)\boldsymbol{t}_m^{(1)} + \boldsymbol{G}_m^{(2)}(\xi)\boldsymbol{t}_m^{(2)}\}\,, \tag{29}$$

其中系数矩阵为

$$\begin{cases} \hat{\boldsymbol{Y}}_m^{(i)} = \displaystyle\int_{-1}^{1} \boldsymbol{T}^{*}(\xi, x_m^{(1)}, x_m^{(2)}, \tilde{\xi})\breve{\omega}_i(\tilde{\xi})\,|\,\boldsymbol{J}_m\,|\,\mathrm{d}\tilde{\xi}\,, \\ \boldsymbol{G}_m^{(i)} = \displaystyle\int_{-1}^{1} \boldsymbol{U}^{*}(\xi, x_m^{(1)}, x_m^{(2)}, \tilde{\xi})\breve{\omega}_i(\tilde{\xi})\,|\,\boldsymbol{J}_m\,|\,\mathrm{d}\tilde{\xi}\,, \end{cases} \tag{30}$$

$$\begin{cases} \mathrm{d}\Gamma_m = |\,\boldsymbol{J}_m\,|\,\mathrm{d}\tilde{\xi}\,, \\ |\,\boldsymbol{J}_m\,| = \sqrt{\left(\dfrac{\partial x_1}{\partial \tilde{\xi}}\right)^{2} + \left(\dfrac{\partial x_2}{\partial \tilde{\xi}}\right)^{2}}\,, \end{cases} \tag{31}$$

$i = 1, 2.M$ 为划分边界单元总数,$|\,\boldsymbol{J}_m\,|$ 为引入无因次坐标变换的 Jacobi 行列式.线性单元为

$$\begin{cases} x = \breve{\omega}_1 x_m^{(1)} + \breve{\omega}_2 x_m^{(2)}\,, \\ u = \breve{\omega}_1 u_m^{(1)} + \breve{\omega}_2 u_m^{(2)}\,, \end{cases} \tag{32}$$

其中,$\breve{\omega}_1 = (1 - \tilde{\xi})/2$,$\breve{\omega}_2 = (1 + \tilde{\xi})/2$,$\breve{\omega}_i (i = 1, 2)$ 为插值函数或形函数,$\Gamma = \Gamma_1 \cup \Gamma_2 \cup \cdots \cup \Gamma_N$,$N$ 为边界节点总数,$\tilde{\xi}$ 为-1 到 1 的无量纲化坐标.

引入记号

$$\begin{cases} \boldsymbol{u}_{m-1}^{(2)} = \boldsymbol{u}_m^{(1)} = \boldsymbol{u}_n\,,\ \boldsymbol{t}_{m-1}^{(2)} = \boldsymbol{t}_m^{(1)} = \boldsymbol{t}_n\,, \\ \hat{\boldsymbol{Y}}_{m-1}^{(2)} + \hat{\boldsymbol{Y}}_m^{(1)} = \boldsymbol{Y}_n\,,\ \boldsymbol{G}_{m-1}^{(2)} + \boldsymbol{G}_m^{(1)} = \boldsymbol{G}_n\,, \end{cases}$$

则式(29)可整理成

$$\begin{cases} \displaystyle\sum_{n=1}^{M} \boldsymbol{Y}_{in}\boldsymbol{u}_n = \sum_{n=1}^{M} \boldsymbol{G}_{in}\boldsymbol{t}_n\,, & i = 1, 2, \cdots, M, \\ \boldsymbol{Y}_{in} = \hat{\boldsymbol{Y}}_{in}\,, & i \neq n, \\ \boldsymbol{Y}_{in} = \hat{\boldsymbol{Y}}_{in} + \hat{\boldsymbol{C}}_i\,, & i = n, \end{cases} \tag{33}$$

其中

$$\hat{\boldsymbol{C}}_i = -\int_{\Gamma} \boldsymbol{T}^{*}(\hat{x}_i, x)\,\mathrm{d}\Gamma\,, \tag{34}$$

$\hat{x}_i$ 为节点i 处的 x 值.仿照边界积分方程的离散格式,将区域内的积分方程离散为

$$\boldsymbol{u}_i = \sum_{n=1}^{N} \boldsymbol{G}_{in}\boldsymbol{t}_n - \sum_{n=1}^{N} \hat{\boldsymbol{Y}}_{in}\boldsymbol{u}_n, \qquad i = 1,2,\cdots,N. \tag{35}$$

利用式(33)计算出各边界节点处的物理量,再把求解的物理量代入式(35),并计算出相应内点的系数矩阵 $\boldsymbol{G}_{in}$ 及 $\hat{\boldsymbol{Y}}_{in}$, 即可计算出区域内任意一点的位移、应力及应变值.

4 数值实例

取二十面体 Al-Pd-Mn 准晶的弹性参数[16] λ = 74.9 GPa, μ = 72.4 GPa, K_1 = 125 MPa, K_2 = − 50 MPa, $R = \sqrt{0.1\mu K_1}$.定义声子场应力集中系数为[34]

$$\chi = \sigma_{\max}/\sigma_{\mathrm{n}}, \tag{36}$$

其中, $\sigma_{\max}$ 为孔边应力的最大值,σ_{n} 为边界施加的载荷大小,应力集中系数可以用来表示含孔板受拉伸时的应力集中程度.如果没有特殊说明,取 a = 0.1 m,b = 0.05 m, 边界施加的载荷均为 1 GPa .

4.1 有限大板与无限大板应力比较

考虑图 1 所示的构型,含椭圆孔有限大二十面体准晶板平面弹性问题声子场和相位子场在单向拉伸时应力的解析解为[16]

$$\begin{cases} \boldsymbol{\phi} = x_1\boldsymbol{t}_2^{\infty} - x_2\boldsymbol{t}_1^{\infty} - \mathrm{Re}\{\boldsymbol{B}\langle\zeta_\alpha^{-1}\rangle\boldsymbol{B}^{-1}(a\boldsymbol{t}_2^{\infty} - \mathrm{i}b\boldsymbol{t}_1^{\infty})\}, \\ [\sigma_{i1}, H_{i1}] = \dfrac{\partial\boldsymbol{\phi}}{\partial x_2}, \ [\sigma_{i2}, H_{i2}] = \dfrac{\partial\boldsymbol{\phi}}{\partial x_1}, \end{cases} \tag{37}$$

其中, $\boldsymbol{t}_1^{\infty}$ = [0,0,0,0,0,0]$^{\mathrm{T}}$ 和 $\boldsymbol{t}_2^{\infty}$ = [0,1 GPa,0,0,0,0]$^{\mathrm{T}}$ 为无限大板在无穷远处施加的载荷,与图 2 有限大试样施加的载荷条件一致.通过式(36)和式(37)求得无限大板椭圆孔边的应力集中系数$\chi \approx 4.935$.

对于有限大板,给定边界条件:

$$\begin{cases} t_1 = 0,\ t_2 = 0,\ h_1 = 0,\ h_2 = 0, & x = \dfrac{W}{2},\ y \in \left(0,\dfrac{H}{2}\right) \cup \left(-\dfrac{H}{2},0\right), \\ t_1 = 0,\ t_2 = 1\ \mathrm{GPa},\ h_1 = 0,\ h_2 = 0, & y = \dfrac{H}{2},\ x \in \left(0,\dfrac{W}{2}\right) \cup \left(-\dfrac{W}{2},0\right), \\ t_1 = 0,\ u_2 = 0,\ h_1 = 0,\ w_2 = 0, & x = \dfrac{W}{2},\ y = 0, \\ u_1 = 0,\ t_2 = 1\ \mathrm{GPa},\ h_2 = 0,\ w_1 = 0, & x = 0,\ y = \dfrac{H}{2}, \end{cases} \tag{38}$$

下边界和右边界为对称边界,椭圆孔边界已考虑在基本解内.

孔边应力集中系数随 W 和 H 的变化如图 3 所示.对经典板采用同样方法进行测试,固定 $W/a \geqslant 100$,当 $H/a \geqslant 185$ 时,有限大板边界元解与无限大板解析解吻合较好.取 H/a = 200,W/a = 100, 准晶有限大板边界元解“.”与无限大板解析解“−”结果对比如图 4 所示.

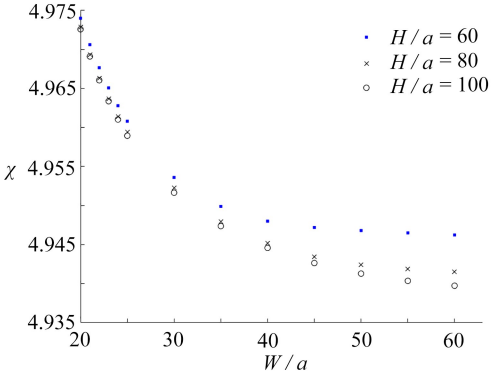

(a) $H/a \in \{60,80,100\}$

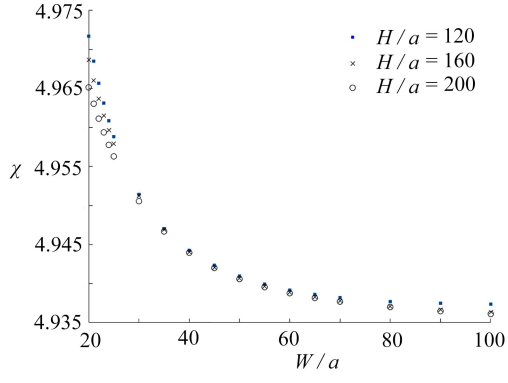

(b) $H/a \in \{120,160,200\}$

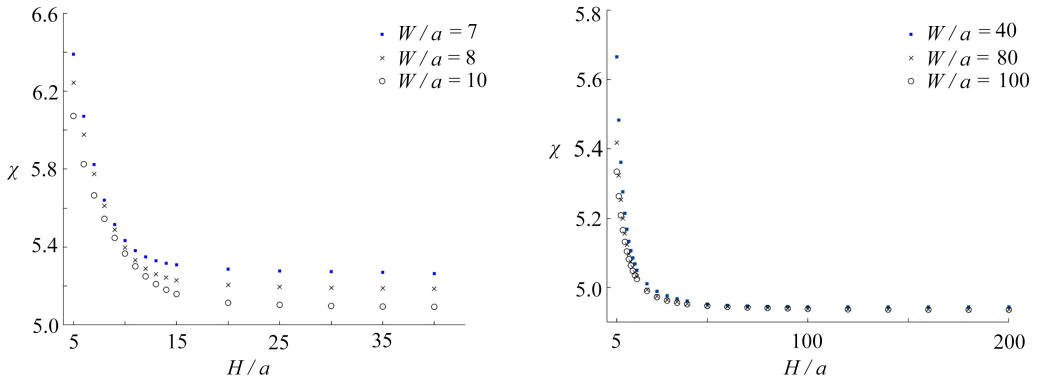

(c) $W/a \in \{7,8,10\}$ (d) $W/a \in \{40,80,100\}$

图 3 声子场应力集中系数随板尺寸的变化

Fig. 3 The variations of phonon stress concentration coefficients with plate sizes

由于图 2 所示构型最大应力分别发生在点 A 及点 B[34],声子场应力(σ_{11} 和 σ_{22}) 及相位子场应力(H_{11} 及 H_{22}) 关于 θ 轴对称,且点 A 及点 B 的有效应力是 σ_{22} 和 H_{22}.因此,本文主要分析声子场应力 σ_{22} 和相位子场应力 H_{22}.

取 $W/a = 8$,$H/a = 40$, 声子场应力 σ_{22} 和相位子场应力 H_{22} 的有限大板边界元解“.”与无限大板解析解“-”结果对比如图 5 所示.由图可见,有限大板与无限大板的孔边应力结果不一致,说明不能用无限大板的解析解分析有限大板问题,此时,可对含椭圆孔有限大板进行边界元分析.

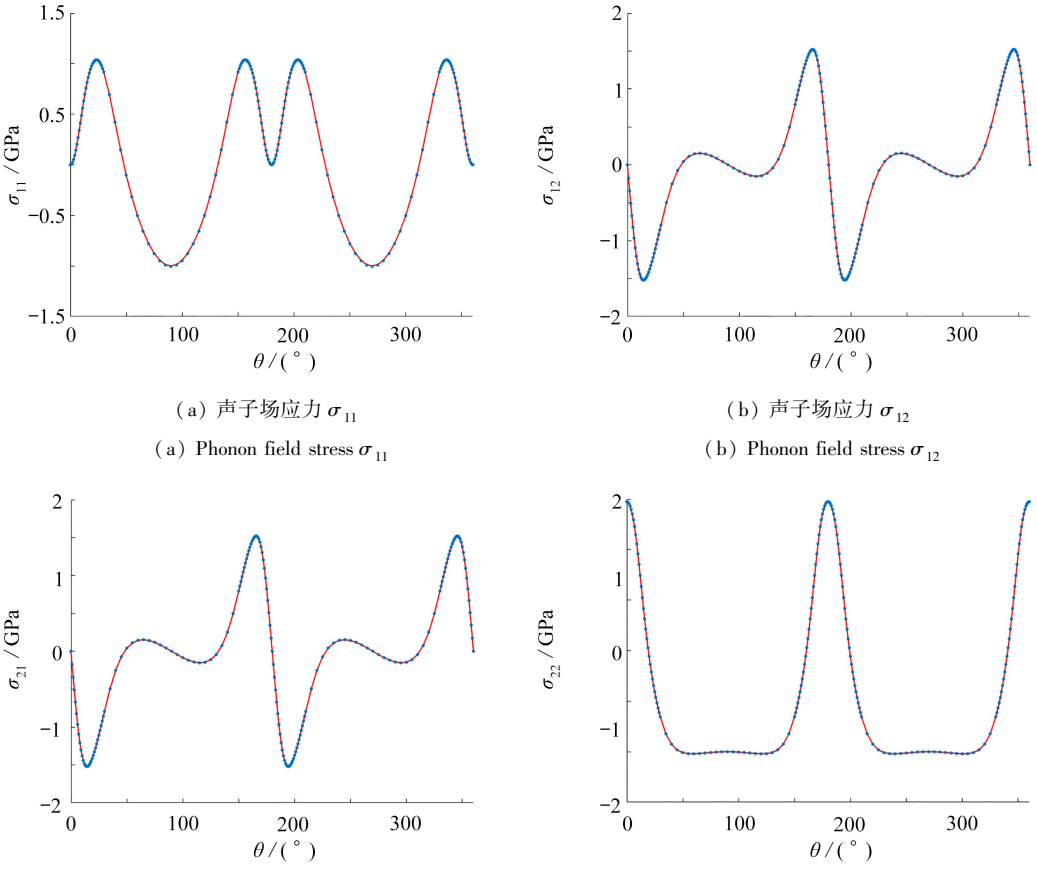

(a) 声子场应力 σ_{11} (b) 声子场应力 σ_{12}

(a) Phonon field stress σ_{11} (b) Phonon field stress σ_{12}

(c) 声子场应力 σ_{21} (d) 声子场应力 σ_{22}

(c) Phonon field stress σ_{21} (d) Phonon field stress σ_{22}

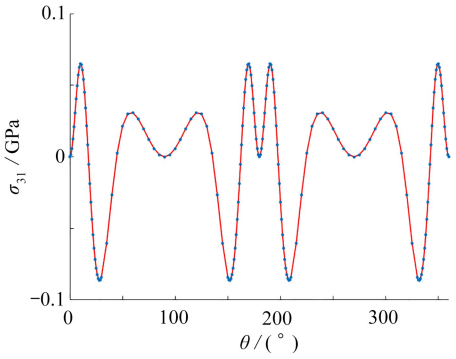

(e) 声子场应力 σ_{31}

(e) Phonon field stress σ_{31}

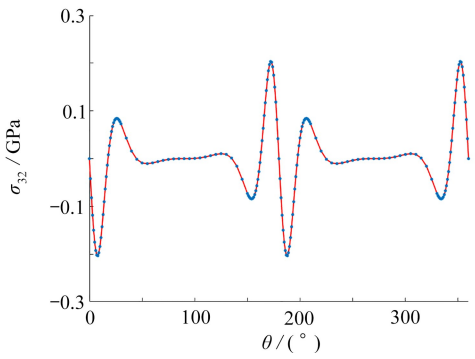

(f) 声子场应力 σ_{32}

(f) Phonon field stress σ_{32}

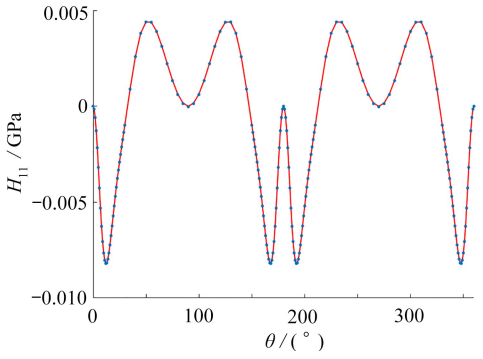

(g) 相位子场应力 H_{11}

(g) Phason field stress H_{11}

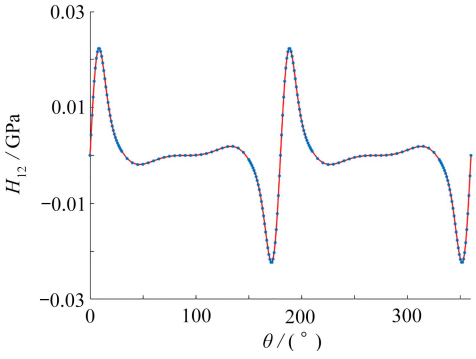

(h) 相位子场应力 H_{12}

(h) Phason field stress H_{12}

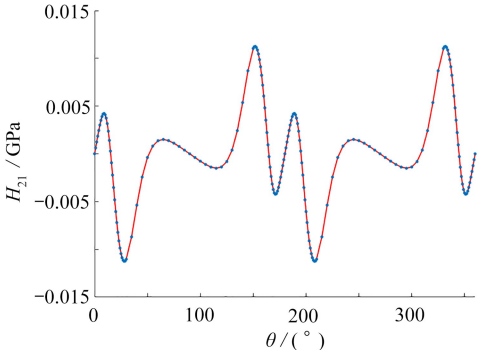

(i) 相位子场应力 H_{21}

(i) Phason field stress H_{21}

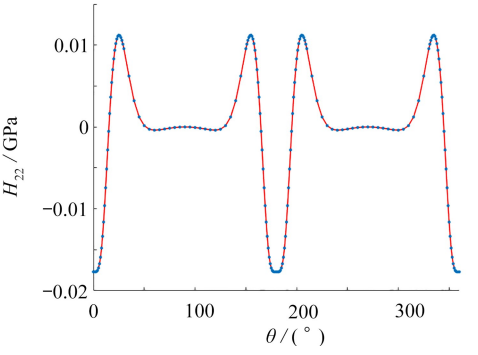

(j) 相位子场应力 H_{22}

(j) Phason field stress H_{22}

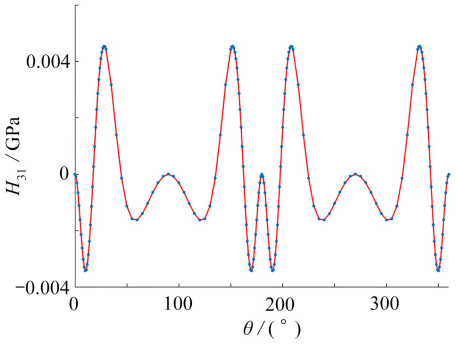

(k) 相位子场应力 H_{31}

(k) Phason field stress H_{31}

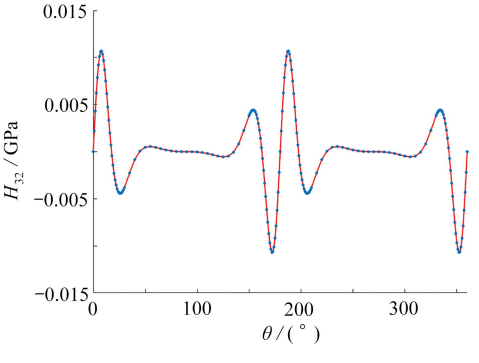

(l) 相位子场应力 H_{32}

(l) Phason field stress H_{32}

图 4 边界元解与无限大板解析解对比 (H/a = 200, W/a = 100)

Fig. 4 Comparison of the boundary element solution and the infinite plate analytical solution (H/a = 200, W/a = 100)

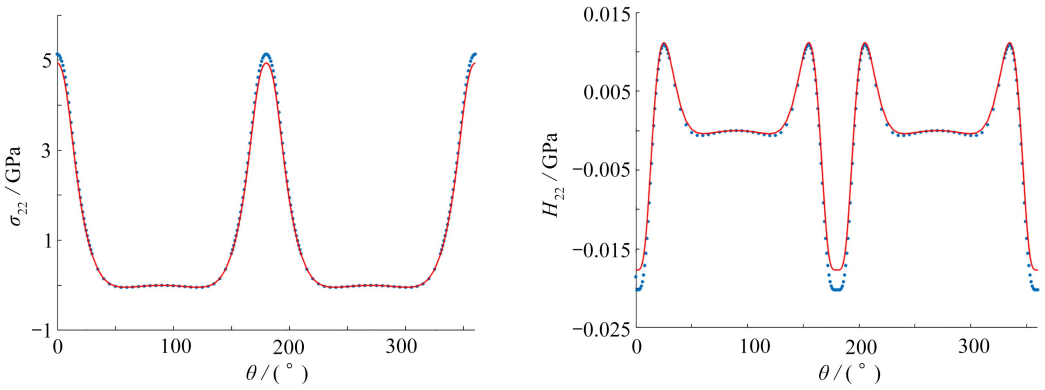

(a) 声子场应力 σ_{22} (b) 相位子场应力 H_{22}

(a) Phonon field stress σ_{22} (b) Phason field stress H_{22}

图 5 边界元解与无限大板解析解对比 ($H/a = 40$, $W/a = 8$)

Fig. 5 Comparison of the boundary element solution and the infinite plate analytical solution ($H/a = 40$, $W/a = 8$)

4.2 孔口尺寸对孔边应力的影响

取板宽 $W = 1$ m,板高 $H = 3$ m,椭圆长短半轴 a 与 b 对孔边应力 σ_{22} 和 H_{22} 的影响如图 6、7 所示.

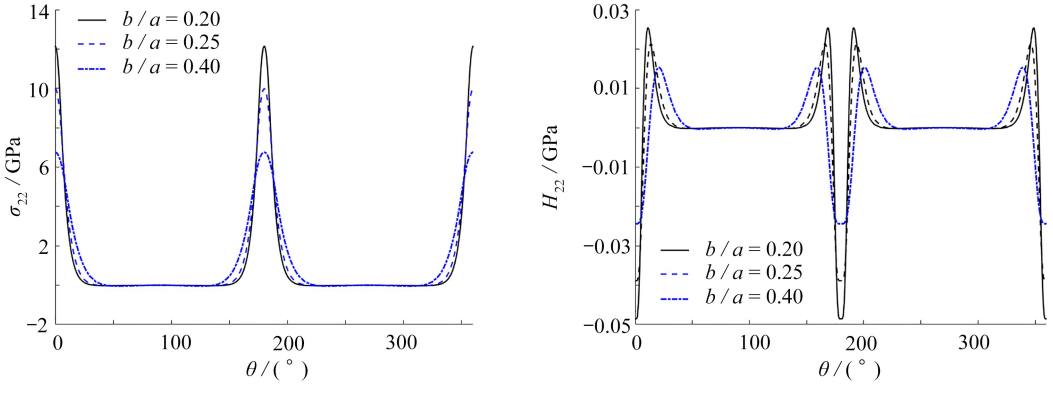

(a) 声子场应力 σ_{22} (b) 相位子场应力 H_{22}

(a) Phonon field stress σ_{22} (b) Phason field stress H_{22}

图 6 取 $a = 0.2$ m,孔边应力值随 b 的变化情况

Fig. 6 For $a = 0.2$ m, the changes of hole edge stresses with b

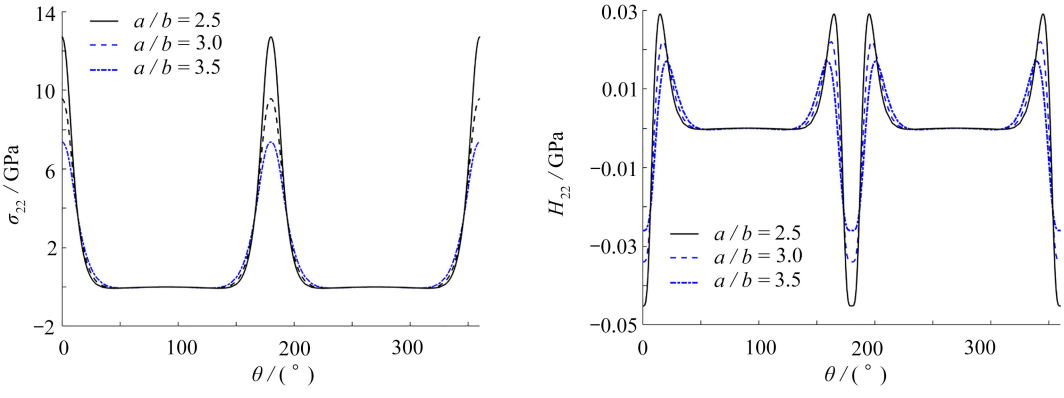

(a) 声子场应力 σ_{22} (b) 相位子场应力 H_{22}

(a) Phonon field stress σ_{22} (b) Phason field stress H_{22}

图 7 取 $b = 0.1$ m,孔边应力值随 a 的变化情况

Fig. 7 For $b = 0.1$ m, the changes of hole edge stresses with a

由图 6 和图 7 可以看出:固定 a,椭圆孔边声子场和相位子场的应力随着 b 的增大而减小;固定 b,声子场和相位子场的应力随着 a 的增大而增大.

4.3 椭圆孔方向与应力集中系数的关系

取板宽 W = 1 m,板高 H = 3 m.图 8 所示的椭圆孔长轴沿逆时针向拉伸方向旋转 α, 图 9 为旋转角度对孔边应力的影响,表 1 为旋转角度对应力集中系数的影响.当长轴与拉伸方向的夹角取不同值时,声子场应力集中系数变化如表 1 所示.

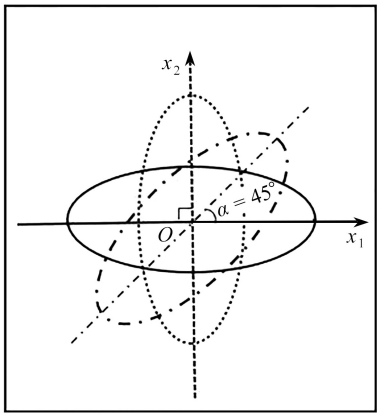

图 8 椭圆孔旋转构型

Fig. 8 The configuration diagram of the elliptic hole rotation

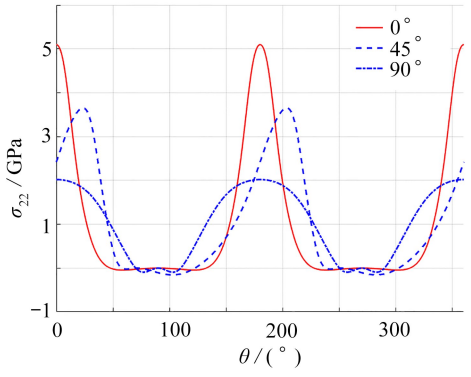

(a) 声子场应力 $\sigma_{22}(\alpha = 0°,45°,90°)$

(a) Phonon field stress $\sigma_{22}(\alpha = 0°,45°,90°)$

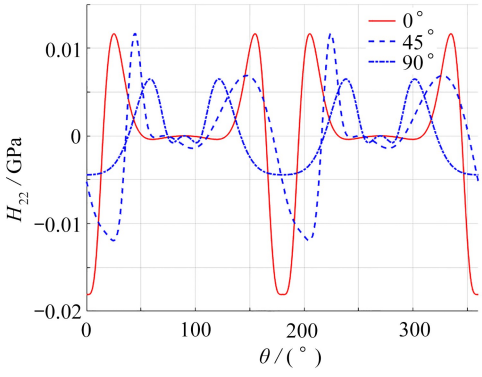

(b) 相位子场应力 $H_{22}(\alpha = 0°,45°,90°)$

(b) Phason field stress $H_{22}(\alpha = 0°,45°,90°)$

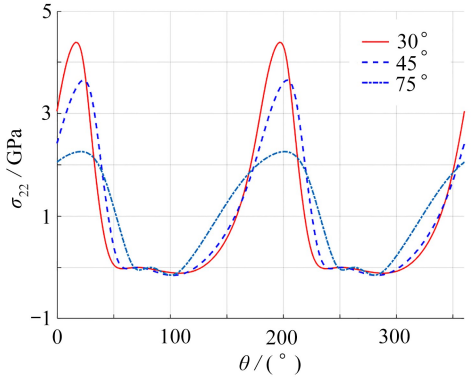

(c) 声子场应力 $\sigma_{22}(\alpha = 30°,45°,75°)$

(c) Phonon field stress $\sigma_{22}(\alpha = 30°,45°,75°)$

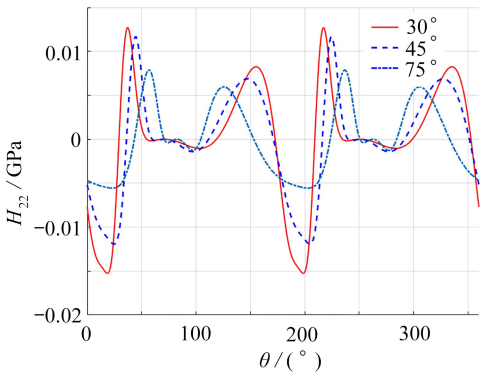

(d) 相位子场应力 $H_{22}(\alpha = 30°,45°,75°)$

(d) Phason field stress $H_{22}(\alpha = 30°,45°,75°)$

图 9 椭圆孔边应力随 α 的变化情况

Fig. 9 The changes of hole edge stresses with α

表 1 应力集中系数随 α 的变化情况

Table 1 The change of the stress concentration coefficient with α

	α/(°)				
	0	15	45	75	90
stress concentration coefficient	5.098 2	4.767 9	3.651 6	2.258 2	2.018 6

由图 9 和表 1 可知,在椭圆沿着其长轴由水平方向向垂直方向旋转的过程中,应力集中系数变小,即椭圆应力集中得到缓解.当椭圆孔的长轴与拉伸方向垂直时,应力集中系数最大;当椭圆孔的长轴与拉伸方向平行时,应力集中系数最小.

4.4 椭圆孔退化到裂纹

考虑图 1 所示构型,取 $b = 0$, 利用声子场应力强度因子

$$K_{\mathrm{I}}^{\sigma} = \lim_{x_1 \to a} \sqrt{2\pi\ (x_1 - a)}\, \sigma_{22} \tag{39}$$

及相位子场应力强度因子

$$K_{\mathrm{I}}^{H} = \lim_{x_1 \to a} \sqrt{2\pi\ (x_1 - a)}\, H_{22}, \tag{40}$$

计算裂纹尖端的应力强度因子随 $2a/W$ 的变化,如图 10 所示.

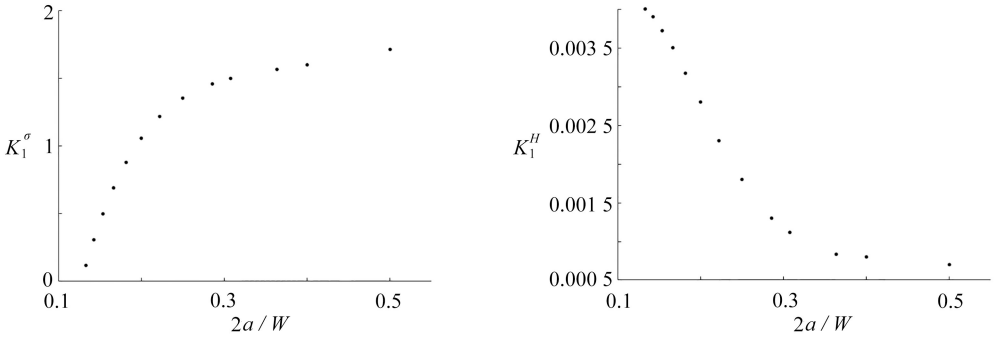

(a) 声子场应力强度因子 (b) 相位子场应力强度因子

(a) The stress intensity factor of the phonon field (b) The stress intensity factor of the phason field

图 10 应力强度因子随 $2a/W$ 的变化情况

Fig. 10 The variation of stress intensity factor with $2a/W$

由图 10 可知,声子场裂纹尖端的应力强度因子随着 $2a/W$ 的增大而增大,相位子场裂纹尖端的应力强度因子随着 $2a/W$ 的增大而减小,且从图中可以看出,声子场裂纹尖端的应力强度因子远大于相位子场裂纹尖端的应力强度因子.

5 结 论

1) 有限大板孔边应力随着板尺寸的增大而减小,且垂直拉伸力方向的板宽 W 的变化对孔边应力的影响小于平行拉伸力方向的板高 H 的变化对孔边应力的影响,即板尺寸沿外力加载方向的变化对孔边应力的影响程度大.当板尺寸与椭圆孔尺寸的比值大于下限值时,可以用无限板孔边应力的解析表达式对有限板进行相应的分析;否则,用边界元法对有限板进行孔边应力分析.

2) 椭圆孔边应力集中系数随 a/b 的增大而增大.即椭圆孔的形状对于材料的力学性质有重要影响,在准晶构件设计时需加以考虑.

3) 椭圆孔方向的变化对孔边应力集中系数产生影响.长轴垂直拉伸方向的椭圆孔逆时针倾斜会引起主应力线变稀疏.这表明在实际工程设计中,应尽量调整椭圆孔的方向,避免长轴与拉伸方向垂直,从而减小应力集中系数,提高构件的强度和稳定性.

4) 含椭圆孔的构件,应力集中系数随应力集中因素方向的不同而不同.对长轴垂直拉伸方向的椭圆孔沿逆时针倾斜引起主应力线变稀疏,因此,构件设计时若考虑应力集中因素方向的选择,应力集中程度有可能减弱.

5) 试样尺寸变化对准晶声子场孔边应力的影响比对弹性板的影响大,这是由于相位子场的出现产生了一定影响.同时,试样尺寸的变化对声子场孔边应力的影响比对相位子场孔边应力的影响大.

本文利用边界元法对图 1 所示的二十面体准晶有限大板平面弹性问题的椭圆孔边应力进行分析,为工程构件设计时简单改进应力集中因素,降低应力集中程度提供了参考.

致谢 本文作者衷心感谢内蒙古师范大学基本科研业务费专项资金(2022JBXC03)以及内蒙古师范大学研究生科研创新基金(CXJJS22099)对本文的资助.

参考文献(References):

[1] YANG W G, DING D H, WANG R H, et al. Thermodynamics of equilibrium properties of quasicrystals[J]. *Zeitschrift für Physik B: Condensed Matter*, 1997, **100**: 447-454.

[2] 范天佑. 准晶数学弹性理论及应用[M]. 北京: 北京理工大学出版社, 1999.(FAN Tianyou. *Quasicrystal Mathematical Elasticity Theory and Its Application*[M]. Beijing: Beijing Institute of Technology Press, 1999.(in Chinese))

[3] 祝爱玉. 三维准晶弹性高阶偏微分方程的解析解和准晶的弹性动力学研究[D]. 北京: 北京理工大学, 2009.(ZHU Aiyu. Analysis solutions of high order partial differential equations of three-dimentional quasicrystals in elasticity and elasto-hydro dynamics of quasicrystals[D]. Beijing: Beijing Institute of Technology, 2009.(in Chinese))

[4] HWU C, YEN W J. Green's functions of two-dimensional anisotropic plates containing an elliptic hole[J]. *International Journal of Solids and Structures*, 1991, **27**(13): 1705-1719.

[5] 舒小敏, 李坚. 基于边界元法求解三维弹性摩擦接触问题[J]. 计算力学学报, 2022,**39**(5): 557-565.(SHU Xiaomin, LI Jian. Solving 3D elastic friction contact problem by boundary element method[J]. *Chinese Journal of Computational Mechanics*, 2022, **39**(5): 557-565.(in Chinese))

[6] XU X L, RAJAPAKSE R. Boundary element analysis of piezoelectric solids with defects[J]. *Composites Part B: Engineering*, 1998, **29**(5): 655-669.

[7] LIANG Y C, HWU C. Electromechanical analysis of defects in piezoelectric materials[J]. *Smart Materials and Structures*, 1996, **5**(3): 314-320.

[8] 袁彦鹏. 准晶材料平面断裂问题分析[D]. 郑州: 郑州大学, 2018.(YUAN Yanpeng. Analysis of plane fracture problem of quasicrystal[D]. Zhengzhou: Zhengzhou University, 2018.(in Chinese))

[9] 陈帅. 一维六方准晶复合材料平面断裂问题研究[D]. 郑州: 郑州大学, 2019.(CHEN Shuai. Study on plane fracture problem of one-dimensional hexagonal quasicrystal bi-material[D]. Zhengzhou: Zhengzhou University, 2019.(in Chinese))

[10] 潘先云, 余江鸿, 周枫林. 非齐次弹性力学问题双互易边界元方法研究[J]. 应用数学和力学, 2022, **43**(9): 1004-1015.(PAN Xianyun, YU Jianghong, ZHOU Fenglin. Research on the dual reciprocity boundary element method for non-homogeneous elasticity problems[J]. *Applied Mathematics and Mechanics*, 2022, **43**(9): 1004-1015.(in Chinese))

[11] 翟婷, 马园园, 赵雪芬. 三维二十面体准晶圆弧形界面刚性线的平面弹性问题[J/OL]. 应用力学学报, 2023[2023-12-12]. https://kns.cnki.net/kcms/detail//61.1112.O3.20230223.1117.004.html.(ZHAI Ting, MA Yuanyuan, ZHAO Xuefen. The plane elasticity problem of circular arc interface rigid lines in three-dimensional icosahedral quasicrystals[J/OL]. *Chinese Journal of Applied Mechanics*, 2023[2023-12-12]. https://kns.cnki.net/kcms/detail//61.1112.O3.20230223.1117.004.html.(in Chinese))

[12] WANG J B, MANCINI L, WANG R, et al. Phonon-and phason-type spherical inclusions in icosahedral quasicrystals[J]. *Journal of Physics: Condensed Matter*, 2003, **15**(24): L363- L370.

[13] FAN T Y, GUO L H. The final governing equation and fundamental solution of plane elasticity of icosahedral quasicrystals[J]. *Physics letters A*, 2005, **341** (1/4): 235-239.

[14] DING D H, YANG W G, HU C Z, et al. Generalized elasticity theory of quasicrystals[J]. *Physical Review B*, 1993, **48**(10): 7003-7010.

[15] GAO Y, RICOEUR A, ZHANG L. Plane problems of cubic quasicrystal media with an elliptic hole or a crack [J]. *Physics Letters A*, 2011, **375**(28/29): 2775-2781.

[16] LI L H, LIU G T. Stroh formalism for icosahedral quasicrystal and its application[J]. *Physics Letters A*, 2012, **376**(28/29): 987-990.

[17] YANG L Z, ANDREAS R, HE F M, et al. Finite size specimens with cracks of icosahedral Al-Pd-Mn quasicrystals[J]. *Chinese Physics B*, 2014, **23**(5): 056102.

[18] LI L H. Generalized 2D problem of icosahedral quasicrystals containing an elliptic hole[J]. *Chinese Physics B*, 2013, **22**(11): 116101.

[19] QIN Q H. Thermoelectroelastic Green's function for a piezoelectric plate containing an elliptic hole[J]. *Mechanics of Materials*, 1998, **30**(1): 21-29.

[20] 张炳彩, 丁生虎, 张来萍. 一维六方准晶双材料中圆孔边共线界面裂纹的反平面问题[J]. 应用数学和力学, 2022, **43**(6): 639-647.(ZHANG Bingcai, DING Shenghu, ZHANG Laiping. The anti-plane problem of collinear interface cracks emanating from a circular hole in 1D hexagonal quasicrystal bi-materials[J]. *Applied Mathematics and Mechanics*, 2022, **43**(6): 639-647.(in Chinese))

[21] 卢绍楠, 赵雪芬, 马园园. 一维六方压电准晶双材料界面共线裂纹问题[J]. 应用数学和力学, 2023, **44**(7): 809-824.(LU Shaonan, ZHAO Xuefen, MA Yuanyuan. Research on interfacial collinear cracks between 1D hexagonal piezoelectric quasicrystal bimaterials[J]. *Applied Mathematics and Mechanics*, 2023, **44**(7): 809-824.(in Chinese))

[22] 尹姝媛, 周旺民, 范天佑. 八次对称二维准晶中的Ⅱ型裂纹[J]. 应用数学和力学, 2002,**23**(4): 376-380.(YIN Shuyuan, ZHOU Wangmin, FAN Tianyou. A mode Ⅱ crack in a two-dimensional octagonal quasicrystals[J]. *Applied Mathematics and Mechanics*, 2002, **23**(4): 376-380.(in Chinese))

[23] LU P, WILLIAMS W. Green functions of piezoelectric material with an elliptic hole or inclusion[J]. *International Journal of Solids and Structures*, 1998, **35**(7/8): 651-664.

[24] ZHOU Y B, LI X F. Fracture analysis of an infinite 1D hexagonal piezoelectric quasicrystal plate with a penny-shaped dielectric crack[J]. *European Journal of Mechanics A: Solids*, 2019, **76**: 224-234.

[25] KAMEL M, LIAW M. Green's functions due to concentrated moments applied in an anisotropic plane with an elliptic hole or a crack[J]. *Mechanics Research Communications*, 1989, **16**(5): 311-319.

[26] GUO J H, YU J, XING Y M, et al. Thermoelastic analysis of a two-dimensional decagonal quasicrystal with a conductive elliptic hole[J]. *Acta Mechanica*, 2016, **227**(9): 2595-2607.

[27] ZHAO X F, LI X, DING S H. Two kinds of contact problems in three-dimensional icosahedral quasicrystals [J]. *Applied Mathematics and Mechanics*(*English Edition*), 2015, **36**(12): 1569-1580.

[28] WANG X F, FAN T Y, ZHU A Y. Dynamic behaviour of the icosahedral Al-Pd-Mn quasicrystal with a Griffith crack[J]. *Chinese Physics B*, 2009, **18**(2): 709-714.

[29] 吴祥法, 范天佑, 安冬梅. 用路径守恒积分计算平面准晶裂纹扩展的能量释放率[J]. 计算力学学报, 2000, **17**(1): 34-42.(WU Xiangfa, FAN Tianyou, AN Dongmei. Energy release rate of plane quasicrystals with crack determined by path-independent *E*-integral[J]. *Chinese Journal of Computational Mechanics*, 2000, **17**(1): 34-42.(in Chinese))

[30] 吴云龙. 十面体准晶和二十面体准晶动态断裂的有限差分分析[D]. 北京: 北京理工大学, 2013.(WU Yunlong. Finite difference analysis of dynamic fracture in decagonal and icosahedral quasicrystals[D]. Beijing: Beijing Institute of Technology, 2013.(in Chinese))

[31] 杨连枝, 张亮亮, 孙振东, 等. 二十面体准晶的有限元模拟方法[C]//中国力学大会: 2013 论文摘要集. 工程科技 I 辑, 2013.(YANG Lianzhi, ZHANG Liangliang, SUN Zhendong, et al. Finite element simulation of icosahedral quasicrystals[C]//*Chinese Mechanics Congress: 2013 Abstracts Collection. Engineering Technology Series I*, 2013.(in Chinese))

[32] 杨连枝, 何蕃民, 高阳. 二十面体 Al-Pd-Mn 准晶板的断裂行为研究[C]//北京力学会第 20 届学术年会论文集. 北京: 中国学术期刊电子出版社, 2014: 2.(YANG Lianzhi, HE Fanmin, GAO Yang. Study of fracture behavior of icosahedral Al-Pd-Mn quasicrystal slab[C]//*The Proceedings of the 20th Annual Conference of Beijing Society of Theoretical and Applied Mechanics*. Beijing: China Academic Journal Electronic Publishing House, 2014: 2.(in Chinese))

[33] GAUL L, KÖGL M, WAGNER M. *Boundary Element Methods for Engineers and Scientists: an Introductory Course With Advanced Topics*[M]. New York: Springer-Verlag, 2003.

[34] 航空工业部科学技术委员会. 应力集中系数手册[M]. 北京: 高等教育出版社, 1990.(Science and Technology Committee of the Ministry of Aeronautics Industry. *Stress Concentration Factors Handbook*[M]. Beijing: Higher Education Press, 1990.(in Chinese))